Cytokinin Targets Auxin Transport to Promote Shoot Branching[1][OPEN]

Tanya Waldie and Ottoline Leyser[2]

Sainsbury Laboratory, Cambridge University, Cambridge CB2 1LR, United Kingdom

Cytokinin promotes shoot branching by activating axillary buds, but its mechanism of action in Arabidopsis (*Arabidopsis thaliana*) in this process is unclear. We have shown previously that a hextuple mutant lacking a clade of type-A Arabidopsis Response Regulators (ARRs) known to act in cytokinin signaling has reduced shoot branching compared with the wild type. Since these proteins typically act as negative regulators of cytokinin signaling, this is an unexpected result. To explore this paradox more deeply, we characterized the effects of loss of function of the type-B ARR, ARR1, which positively regulates cytokinin-induced gene expression. The *arr1* mutant has increased branching, consistent with a role antagonistic to the type-A ARRs but in apparent conflict with the known positive role for cytokinin in bud activation. We show that the *arr* branching phenotypes correlate with increases in stem auxin transport and steady-state levels of the auxin export proteins PIN3 and PIN7 on the plasma membrane of xylem-associated cells in the main stem. Cytokinin treatment results in an increased accumulation of PIN3, PIN7, and the closely related PIN4 within several hours, and loss of *PIN3*, *PIN4*, and *PIN7* can partially rescue the *arr1* branching phenotype. This suggests that there are multiple signaling pathways for cytokinin in bud outgrowth; one of these pathways regulates PIN proteins in shoots, independently of the canonical signaling function of the *ARR* genes tested here. A hypothesis consistent with the *arr* shoot phenotypes is that feedback control of biosynthesis leads to altered cytokinin accumulation, driving cytokinin signaling via this pathway.

Plant developmental plasticity is exemplified by the diversity in shoot forms seen within a species, which are tuned according to environmental conditions. One process underlying this diversity is differential activation of axillary buds throughout the plant's life cycle, which results in diverse shoot branching habits. The hormonal signaling network controlling bud activity involves auxin, strigolactone (SL), and cytokinin (CK), all of which have well-defined physiological roles, although the molecular mechanisms through which they control bud outgrowth are not yet entirely clear (for review, see Domagalska and Leyser, 2011; Teichmann and Muhr, 2015). It is well established that apical dominance, the inhibitory effect imposed by an actively growing shoot apex on axillary buds, is mediated at least in part by the synthesis and movement of auxin from young expanding leaves into the basipetal polar auxin transport stream (PATS) in the main stem (Thimann and Skoog, 1933; Ljung et al., 2001). Auxin in the PATS does not enter axillary buds to exert this repression and, thus, acts indirectly (Hall and Hillman, 1975; Morris, 1977; Booker et al., 2003). There is a substantial body of evidence supporting two parallel mechanisms for the indirect action of auxin on axillary bud growth (for review, see Domagalska and Leyser, 2011). One is that auxin in the main stem regulates the synthesis of second messengers that move up into the buds and regulate their activity. The other is that stem auxin influences the establishment of canalized auxin flow out of buds into the PATS. According to this canalization-based mechanism, auxin movement begins as a weak flux from the bud, an auxin source, into the main stem PATS, an auxin sink. This flux narrows and strengthens due to positive feedback between auxin flux and the auxin transport machinery (Sachs, 1981; Prusinkiewicz et al., 2009). This process results in the formation of specialized cell files that conduct auxin from source to sink, and this is hypothesized to be required for sustained bud activation. The action of SL and CK in bud activation control can be considered in terms of these two models.

In dicots, SL is thought to act via both mechanisms. Auxin up-regulates the transcription of SL biosynthetic genes in the stem, and SL can move upward into buds, presumably in the transpiration stream (Foo et al., 2001, 2005; Bainbridge et al., 2005; Johnson et al., 2006; Hayward et al., 2009). There, SL modulates the expression of the TEOSINTE BRANCHED1/CYCLOIDEA/PCNA family transcription factor *BRANCHED1* (*BRC1*), an inhibitor of shoot branching (Aguilar-Martínez et al., 2007; Poza-Carrión et al., 2007; Braun et al., 2012; Dun et al., 2012). However, high *BRC1* transcript levels are neither necessary nor sufficient for bud inhibition, and mutant buds lacking *BRC1* can be inhibited by SL (Seale et al., 2017). Furthermore, SL addition can promote branching in an auxin transport-compromised genetic background, demonstrating that this simple second messenger mechanism cannot be the only mode of action for SL (Shinohara et al., 2013). Consistent with this

[1]This work was funded by the European Research Council (no. 294514-EnCoDe) and the Gatsby Charitable Foundation (GAT3272C).

[2] Address correspondence to ol235@cam.ac.uk.

The author responsible for distribution of materials integral to the findings presented in this article in accordance with the policy described in the Instructions for Authors (www.plantphysiol.org) is: Ottoline Leyser (ol235@cam.ac.uk).

T.W. designed, performed, and analyzed the results of all the experiments; T.W. and O.L. co-conceived the research plans, interpreted the results, and wrote the article.

[OPEN]Articles can be viewed without a subscription.

www.plantphysiol.org/cgi/doi/10.1104/pp.17.01691

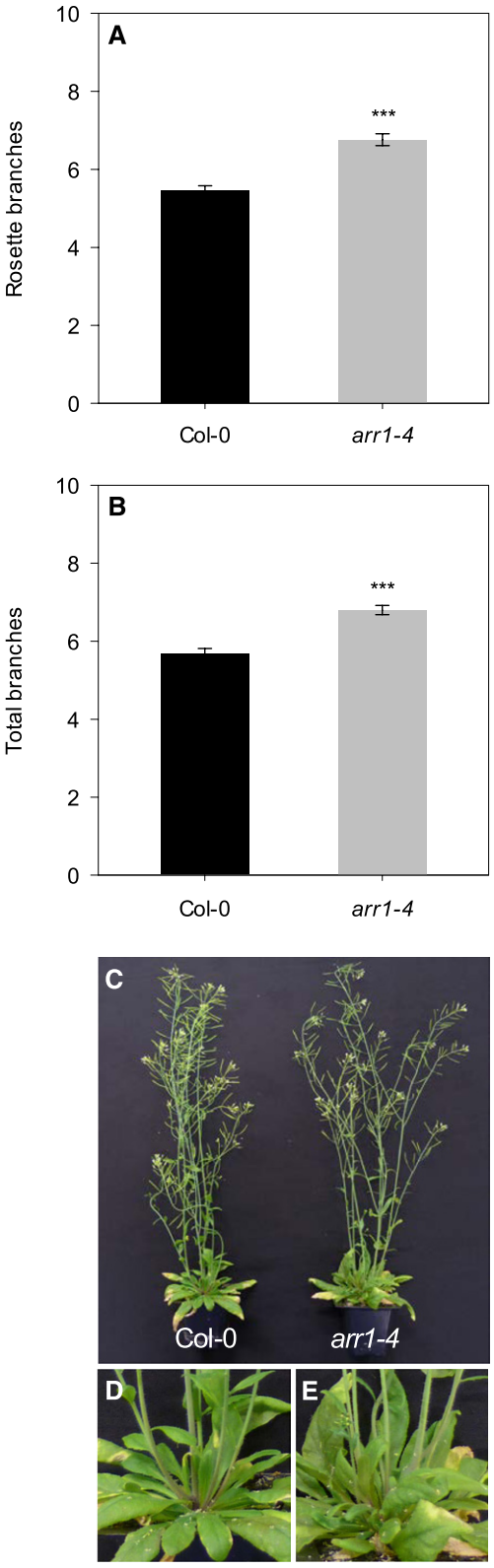

Figure 1. An *ARR1* mutation confers increased shoot branching. A, Rosette branches formed 10 d after primary shoot decapitation in plants grown in short days for 4 weeks and long days for ~3 weeks, as described by Greb et al. (2003) (n = 38–40). B, Total branches (rosette and cauline) formed in Columbia-0 (Col-0) and *arr1-4* plants grown in long days for ~6 weeks (n = 30–31). C to E, Shoot-branching phenotypes of Col-0 and *arr1-4* plants grown in long days for ~7 weeks. Closeup views of the rosettes in C are shown in D (Col-0) and E (*arr1-4*). Error bars indicate SE, and the statistical comparisons shown are between the mutant and the wild type (Mann-Whitney test, ***, $P \leq 0.001$).

idea, SL triggers the rapid removal of the auxin export protein, PIN1, from the plasma membrane (Crawford et al., 2010; Shinohara et al., 2013; Bennett et al., 2016). This effect is sensitive to inhibitors of clathrin-mediated endocytosis but not to the translation inhibitor cycloheximide, suggesting a non-transcriptional mode of action of SL on PIN1 endocytosis. In the context of an auxin transport canalization-based model for bud activation, PIN1 removal can account for the inhibitory effect of SL on shoot branching, since it is predicted to make canalization more difficult to achieve by dampening the feedback between auxin flux and auxin transporter accumulation. Furthermore, when auxin transport is compromised and auxin fluxes are systemically low, the effect of SL on PIN1 endocytosis is predicted to promote branching, as observed (Shinohara et al., 2013).

Half a century before the discovery of SL, one of the earliest described roles for CK in plant development was in bud activation (Wickson and Thimann, 1958). In Arabidopsis (*Arabidopsis thaliana*), basally applied CK can overcome the inhibitory effects of apical auxin on bud activity (Chatfield et al., 2000). Furthermore, *isopentenyl transferase3,5,7* (*ipt3,5,7*) mutants impaired in CK biosynthesis have reduced CK levels and form fewer branches than wild-type plants (Miyawaki et al., 2006; Müller et al., 2015). As for SL, there is good evidence that CK can act as a second messenger for stem auxin. Removal of the shoot apex correlates with increased stem CK levels, and addition of auxin reduces them (Bangerth, 1994; Tanaka et al., 2006). In Arabidopsis, CK is perceived at the endoplasmic reticulum by the HISTIDINE KINASE (AHK) receptor kinase family, which initiates a phosphorelay cascade that targets the large, multiple-member family of ARABIDOPSIS RESPONSE REGULATORs (ARRs) in the nucleus via HISTIDINE PHOSPHOTRANSFER proteins (for review, see Schaller et al., 2015). The ARRs possess an N-terminal phosphoreceiver domain and comprise two subclasses based on the presence (in type-Bs) or absence (in type-As) of a DNA-binding domain. Type-B ARRs directly regulate transcription and function as positive regulators of CK signaling, whereas type-A ARRs typically function as negative regulators. Therefore, it has been widely assumed that CK activates buds by regulating the transcription of relevant genes in the bud, such as *BRC1*. There is good evidence to support this model, since in both pea (*Pisum sativum*) and Arabidopsis, *BRC1* expression is down-regulated by CK (Braun et al., 2012; Dun et al., 2012; Seale et al., 2017). However, CK can promote bud activation in pea *brc1* mutants, demonstrating

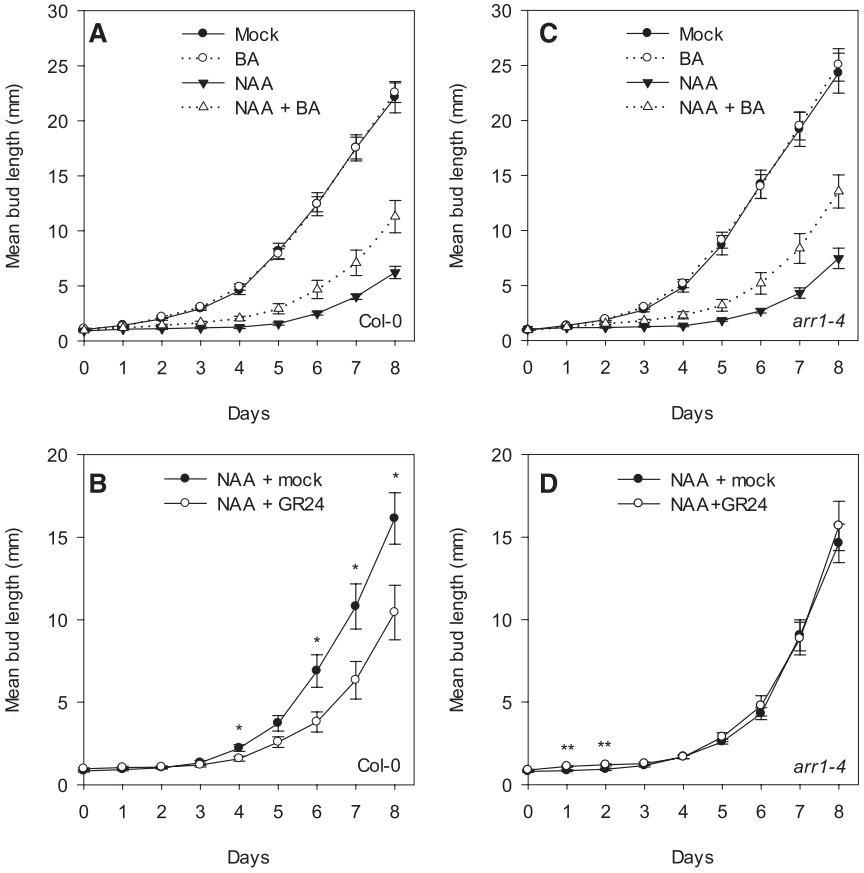

Figure 2. *arr1* buds have wild-type responses to auxin and cytokinin but are resistant to strigolactone. Wild-type (A and C) or *arr1* (B and D) isolated nodal segments bearing one bud were treated for 8 d with mock, 1 μM NAA (apical), 1 μM BA (basal), or combined 1 μM NAA (apical) and 1 μM BA (basal) (n = 18–20; A and B) or with 0.5 μM NAA (apical) or combined 0.5 μM NAA (apical) and 5 μM GR24 (basal) (n = 18–20; C and D). Error bars indicate SE. Statistical comparisons shown were made between NAA and NAA + GR24-treated buds at each time point (Student's t test, *, $P < 0.05$ and **, $P \leq 0.01$).

that CK has *BRC1*-independent effects on the regulation of bud outgrowth (Braun et al., 2012). Furthermore, the Arabidopsis hextuple type-A *arr3,4,5,6,7,15* mutant exhibits reduced bud activation, a phenotype opposite to that predicted, based on the established roles of type-A ARR proteins as negative regulators of transcriptional CK signaling (To et al., 2004; Müller et al., 2015).

To explore this paradoxical result further, we describe here the analysis of the type-B ARR mutant, *arr1*. ARR1 binds to the promoters of CK up-regulated genes, including those induced during CK-triggered bud activation. Therefore, we hypothesized that the *arr1* mutant should show reduced and CK-resistant shoot branching. However, our results demonstrate that *arr1* has increased and CK-responsive shoot branching, suggesting an alternative mechanism for CK-mediated shoot branching control. We provide evidence that the mechanism involves the CK-mediated accumulation of the PIN3, PIN4, and PIN7 auxin transporters.

RESULTS

Type-A and Type-B *arr* Mutations Confer Opposite Shoot-Branching and Auxin Transport Phenotypes

Previously, we found that the hextuple type-A *arr3,4,5,6,7,15* mutant has reduced shoot branching relative to the wild type (Müller et al., 2015). Since type-B ARR family members are known to act antagonistically to type-A ARRs in other CK responses, we investigated shoot branching in the *arr1* loss-of-function mutant. *ARR1* was selected because a group of CK-up-regulated genes in buds possess an *ARR1* response element in their promoters (Müller et al., 2015). In accordance with action antagonistic to type-A ARRs, the type-B *arr1* single mutant has increased branching compared with wild-type controls, forming a mean of 6.8 rosette branches compared with 5.5 in the wild type when decapitated (Fig. 1A; $P < 0.001$) and a mean of 6.8 branches compared with 5.7 in the wild type when intact (Fig. 1, B–E; $P < 0.001$).

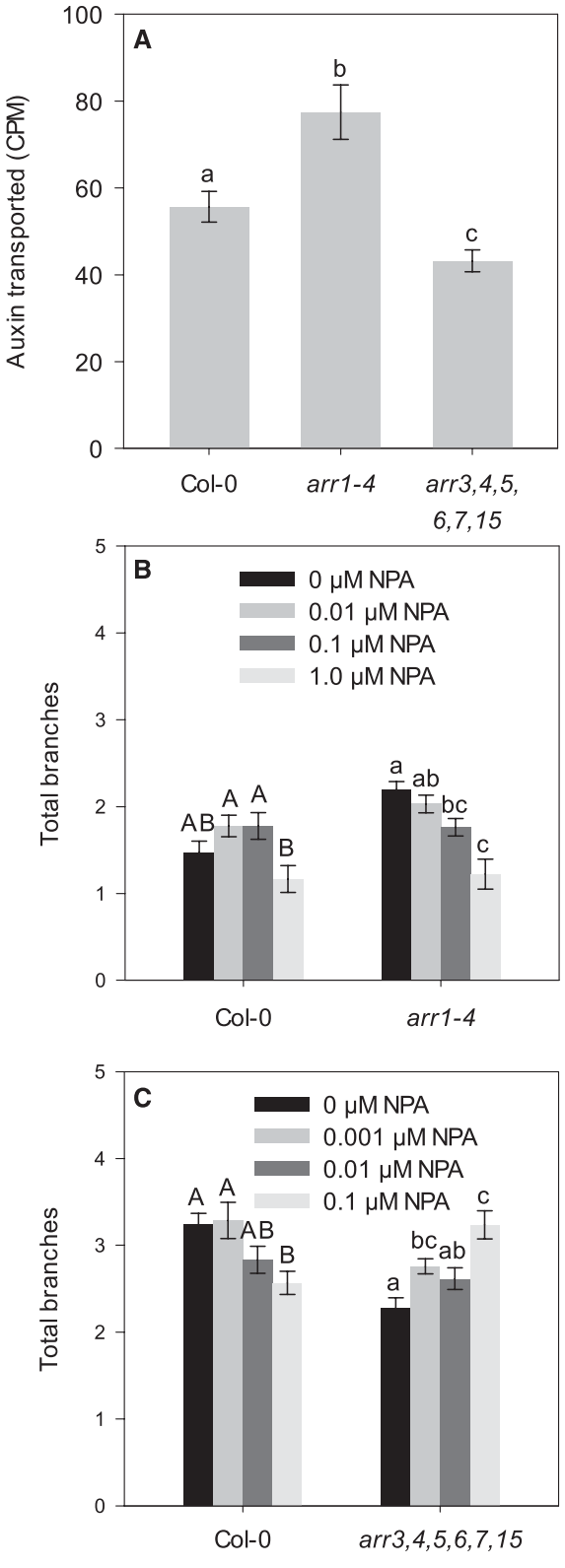

Figure 3. Type-A and type-B *arr* mutant branching phenotypes are associated with altered auxin transport. A, Amount of apically applied [^{14}C]indole-3-acetic acid (cpm) transported to the basal end of inflorescence stem internodes from ~6 week-old wild-type, *arr1*, and *arr3,4,5,6,7,15* plants in 6 h (n = 24–32). Different letters denote significant differences (ANOVA, Tukey's b post hoc test, $P < 0.05$). B, NPA dose response of wild-type and *arr1* plants grown for 6 weeks on different concentrations of NPA under sterile conditions (n = 18–42). C, NPA dose response of wild-type and *arr3,4,5,6,7,15* plants grown for 6 weeks on different concentrations of NPA under sterile conditions (n = 13–24). Error bars indicate SE. For B and C, letters denote significant differences within a genotype (Kruskal-Wallis H test, $P < 0.05$).

Buds on isolated nodal stem segments from *arr3,4,5,6,7,15* plants treated with apical auxin were shown previously to be resistant to the effects of basal CK and slightly resistant to basal SL (Müller et al., 2015). The same isolated nodal assay system was used to assess bud hormone responses in *arr1* (Chatfield et al., 2000; Crawford et al., 2010). Briefly, small nodal stem segments, each bearing an inactive cauline bud, were excised from bolting inflorescences. The apical end of the stem was embedded in an agar block supplemented with synthetic auxin (1-naphthalene acetic acid [NAA]) or a control solution. The basal end of the stem was embedded in an agar block supplemented with CK (6-benzylaminopurine [BA]), SL (rac-GR24), or a control solution (hereafter referred to as apical NAA, basal BA, and basal GR24 treatments). The kinetics of outgrowth in mock-treated *arr1* buds was similar to that in the wild type (Fig. 2, A and B). For both genotypes, apical NAA delayed bud activation by ~3 d. The response of *arr1* to BA also was similar to that of the wild type, where basal BA alone had little effect compared with mock treatment, but basal BA could overcome the inhibitory effect of apical NAA and activate buds. As reported previously, basal GR24 prolonged the inhibitory effect of apical NAA in the wild type, but *arr1* buds were resistant to basal GR24 under these conditions (Fig. 2, C and D). To assess whether this altered GR24 response extended beyond isolated nodes, whole plants were grown under axenic conditions on ATS medium supplemented with GR24, as described by Crawford et al. (2010). Branching in wild-type plants was significantly inhibited by 1 µM GR24, whereas 5 µM was required for significant branch inhibition in *arr1* plants (Supplemental Fig. S1).

The altered GR24 responses of *arr1* single and *arr3,4,5,6,7,15* hextuple mutants raise the possibility that *arr* mutations may affect auxin transport processes in the shoot. Therefore, we compared bulk auxin transport in wild-type, type-A, and type-B *arr* mutant stem segments, as described previously (Bennett et al., 2016). Compared with the wild type, *arr1* transported 40% more auxin ($P < 0.01$) and *arr3,4,5,6,7,15* transported 23% less ($P < 0.01$) over the 6 h assay period (Fig. 3A). To determine whether this effect was associated with CK signaling, we also assessed the *ipt3* CK biosynthesis mutant, which we have shown previously to have a reduced shoot branching phenotype (Müller et al., 2015). Similar to *arr3,4,5,6,7,15*, the *ipt3* mutant also exhibited reduced auxin transport (Supplemental Fig. S2). Thus, the degree of shoot branching correlates

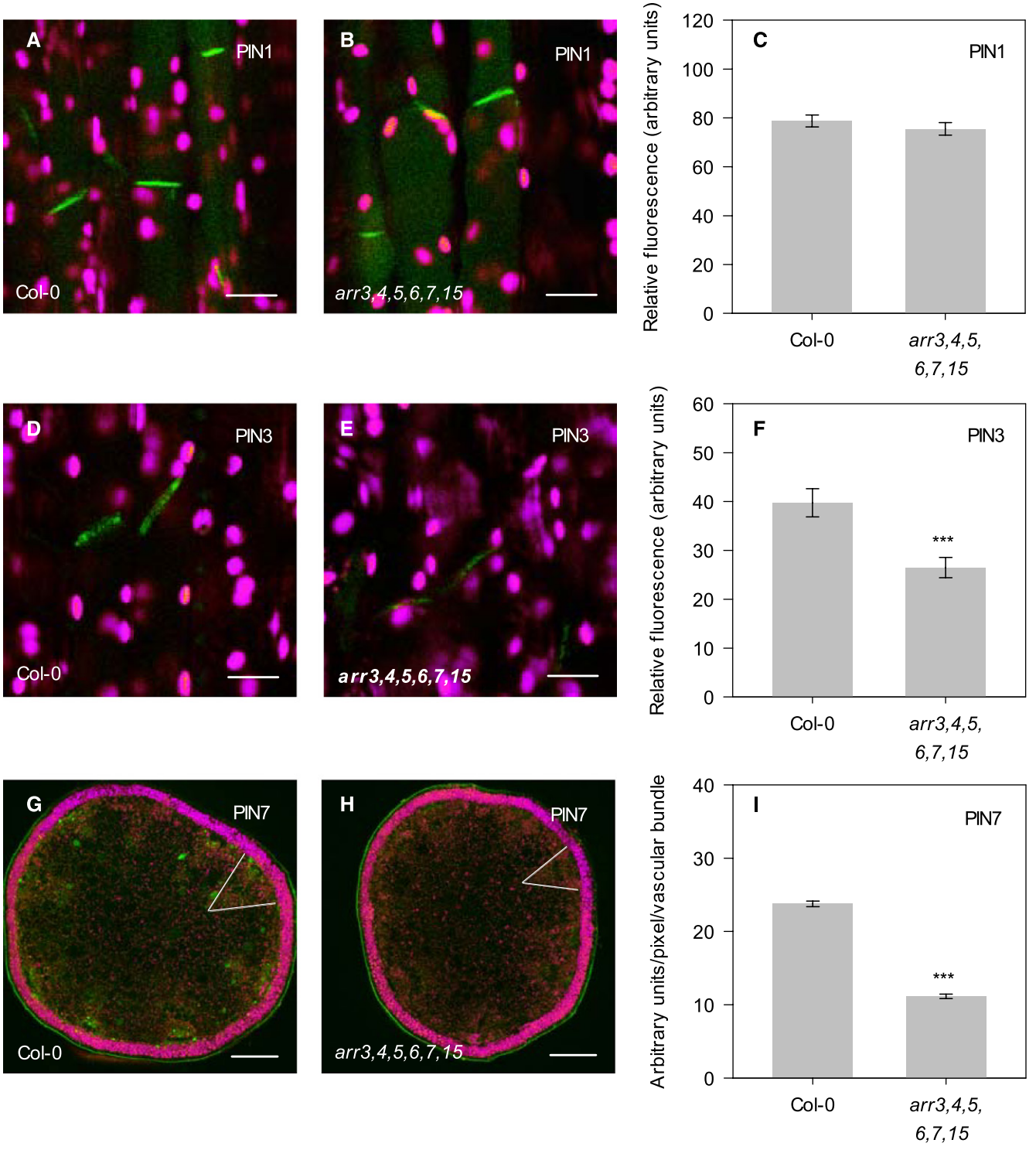

Figure 4. PIN3-GFP and PIN7-GFP accumulation is attenuated in *arr3,4,5,6,7,15* inflorescence stems. A, B, D, E, G, and H, Representative accumulation patterns of PIN1-GFP (A and B), PIN3-GFP (D and E), and PIN7-GFP (G and H) in basal inflorescence internodes of Col-0 (A, D, and G) and *arr3,4,5,6,7,15* (B, E, and H) plants, imaged at ~5 to 6 weeks of age using confocal microscopy. For confocal images, green shows PIN-GFP signal and magenta shows chloroplast autofluorescence. Bars = 10 μm (A, B, D, and E) or 200 μm (G and H). C and F, For PIN1:PIN1-GFP and PIN3:PIN3-GFP, plants were sectioned longitudinally and the amount of GFP signal on the basal plasma membrane was quantified in the xylem parenchyma using at least five cells each from eight independent plants (n = 40). I, For PIN7:PIN7-GFP, plants were sectioned transversely (~2 mm thickness), and the amount of GFP signal was quantified in at least five vascular bundles from five independent plants

positively with bulk auxin transport in the stems of these mutant genotypes.

To test this correlation further, we assessed the shoot branching responses of *arr1* and *arr3,4,5,6,7,15* plants to the auxin transport inhibitor 1-naphthylphthalamic acid (NPA). Plants were grown under axenic conditions on ATS medium supplemented with NPA, as described by Bennett et al. (2006). Significant reductions in branching were observed in *arr1* plants treated with 0.1 μM NPA ($P < 0.05$) and 1 μM NPA ($P < 0.001$; Fig. 3B), consistent with a causative link between auxin transport defects and shoot branching in the *arr1* mutant, similar to the results obtained for SL-deficient mutants (Bennett et al., 2006). In contrast, treatment with 0.1 μM NPA significantly increased branching in *arr3,4,5,6,7,15* ($P < 0.01$; Fig. 3C). This is consistent with the well-established promotive effect of very low auxin transport on branching (Ruegger et al., 1997; Geldner et al., 2003). Taken together, these results suggest that mutations in type-A and type-B ARR family members perturb auxin transport in the shoot, and this contributes to their effects on shoot branching.

CK Signaling Targets PIN Proteins in the Stem

Several PIN proteins contribute to stem auxin transport in Arabidopsis. PIN1 is an important component of the classical PATS and is expressed in a highly polar manner in xylem parenchyma and cambium cells in the stem vasculature. PIN3, PIN4, and PIN7 contribute to PATS and to a less polar route, termed connective auxin transport, which connects surrounding tissues and organs, including axillary buds, to the PATS (Bennett et al., 2016). To determine whether *arr* mutant shoots have alterations in PIN accumulation, we analyzed the steady-state transcript levels of *PIN1*, *PIN3*, *PIN4*, and *PIN7* in *arr1* and *arr3,4,5,6,7,15*. *PIN* transcript levels were analyzed in upper inflorescence internodes of wild-type, *arr1*, and *arr3,4,5,6,7,15* plants usingreverse transcription-quantitative PCR (Supplemental Fig. S3). Apart from a 5-fold increase in *PIN7* transcripts in *arr3,4,5,6,7,15* compared with the wild type ($P < 0.01$), no significant changes were observed, suggesting that the *arr* mutant auxin transport phenotypes do not correlate with alterations in *PIN* transcript abundance in inflorescence stems.

In the absence of correlative changes in *PIN* transcription, we assessed PIN protein localization and abundance using established PIN-GFP reporter lines crossed into the type-A and -B *arr* mutant backgrounds. PIN-GFP accumulation patterns were analyzed in longitudinal or transverse sections of basal inflorescence internodes (the inflorescence internode located directly above the rosette and farthest from the shoot apex) and imaged using confocal microscopy. In *arr3,4,5,6,7,15* mutants, the amount of PIN1-GFP on the basal plasma membrane (the rootward-facing membrane farthest from the shoot apex) of xylem parenchyma cells was unchanged compared with the wild type (Fig. 4, A–C). In contrast, the amount of PIN3-GFP on the basal plasma membrane of xylem parenchyma cells was reduced by ~25% in *arr3,4,5,6,7,15* compared with the wild type ($P < 0.001$; Fig. 4, D–F). As PIN7-GFP typically shows a broad, cross-stem pattern of accumulation in young wild-type internodes, and PIN7-GFP was not detectable on the basal plasma membrane of xylem parenchyma cells in *arr3,4,5,6,7,15*, the PIN7-GFP signal was quantified within vascular bundles in inflorescence stem transverse sections (Fig. 4, G–I). Like PIN3-GFP, PIN7-GFP also was decreased significantly in *arr3,4,5,6,7,15* compared with the wild type ($P < 0.001$). Analysis of the *ipt3* CK synthesis mutant revealed similar patterns of PIN1-GFP and PIN7-GFP accumulation to the *arr3,4,5,6,7,15* mutant, with wild-type levels of PIN1-GFP present on the basal plasma membrane of xylem parenchyma cells and decreased levels of PIN7-GFP within vascular bundles ($P < 0.001$; Supplemental Fig. S4).

Wild type levels of basal plasma membrane-localized PIN1-GFP also were observed in the *arr1* mutant (Fig. 5, A–C). However, in contrast to *arr3,4,5,6,7,15*, PIN3-GFP was increased ~20% in *arr1* inflorescence stems compared with the wild type ($P < 0.05$; Fig. 5, D–F). In transverse sections of young basal *arr1* inflorescence internodes (8–10 cm high), PIN7-GFP was restricted to the outer xylem parenchyma and cambium of vascular bundles, whereas wild-type plants exhibited a brighter and broader accumulation pattern that decreased at later stages, as reported previously (Bennett et al., 2016; Supplemental Fig. S5). In contrast, the accumulation of PIN7-GFP associated with vascular bundles appeared to be slightly higher in *arr1* than in the wild type at later stages of inflorescence development (18–20 cm and 28–30 cm high; Supplemental Fig. S5, C–F). In accordance with this observation, the amount of PIN7-GFP present on the basal plasma membranes of xylem parenchyma cells in longitudinal sections of inflorescence stems was increased ~25% ($P < 0.01$) in *arr1* compared with the wild type (Fig. 5, G–I).

These data suggest that the auxin transport phenotypes of the *arr3,4,5,6,7,15* and *arr1* mutants are due at least in part to differential accumulation of PINs belonging to the PIN3, PIN4, and PIN7 clade in the stem. To assess whether this is a direct effect of CK, we assessed the responses of these PIN proteins to BA treatment. Inflorescence stem segments from wild-type plants were held between two agar blocks supplemented with NAA in the upper block and BA or a control solution in the lower block. After 4 h of treatment, a longitudinal section was made in the basal half of the stem segment, at or near the site of BA treatment, and imaged using confocal microscopy. The

Figure 4. (*Continued.*)
with inflorescence stems stage matched at 24 to 26 cm in height ($n = 25$). Error bars indicate SE, and the statistical comparisons shown were made between the mutant and the wild type (Student's *t* test, ***, $P < 0.001$).

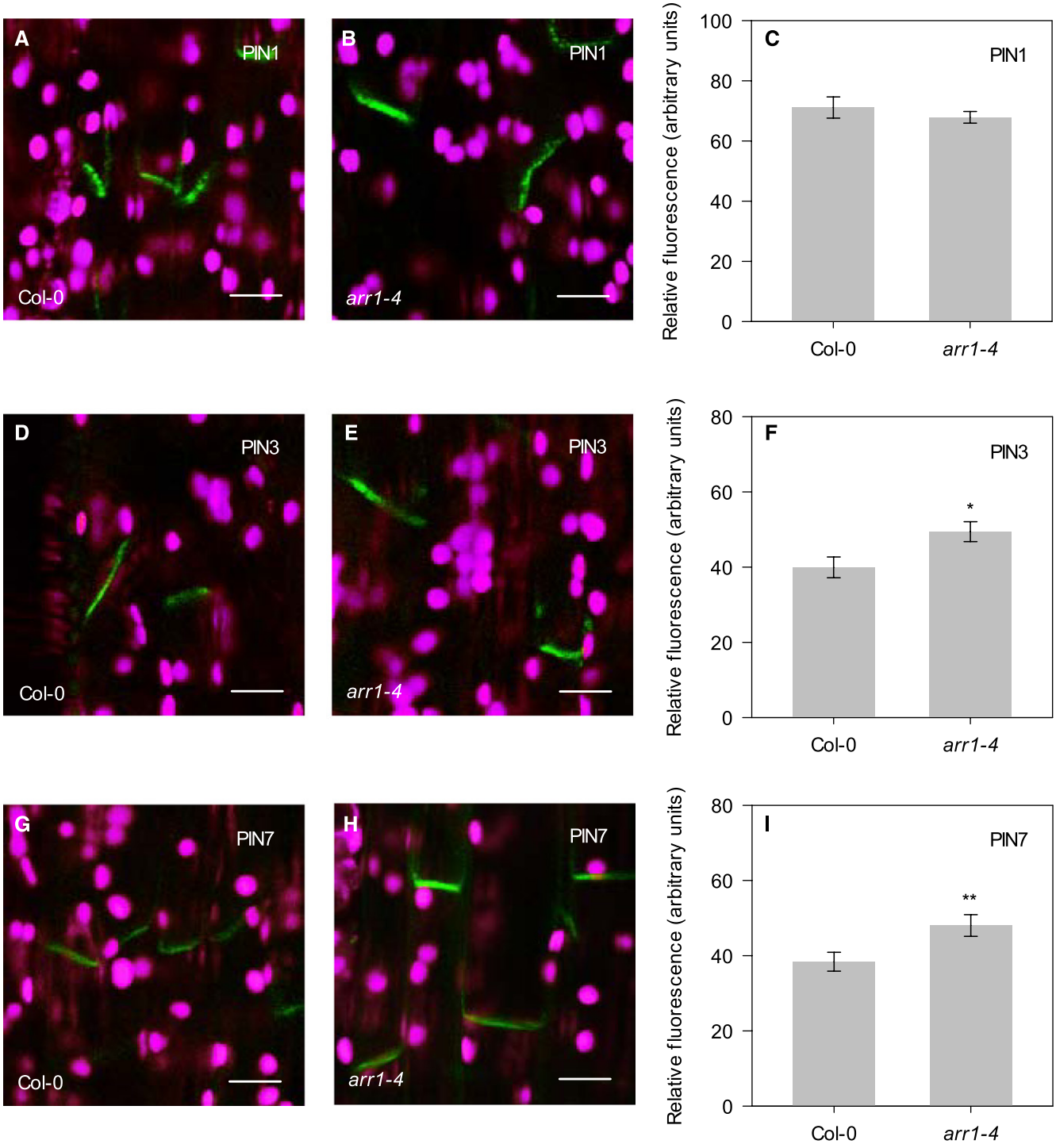

Figure 5. PIN3-GFP and PIN7-GFP accumulation is elevated in *arr1* inflorescence stems. A, B, D, E, G, and H, Representative accumulation patterns of PIN1-GFP (A and B), PIN3-GFP (D and E), and PIN7-GFP (G and H) in basal inflorescence internodes of 4- to 7-week-old Col-0 (A, D, and G) and *arr1* (B, E, and H) plants, sectioned longitudinally and imaged using confocal microscopy. Green shows PIN-GFP signal, and magenta shows chloroplast autofluorescence. Bars = 10 μm. C, F, and I, The amount of GFP signal on the basal plasma membrane was quantified in the xylem parenchyma using at least five cells each from eight independent plants ($n = 40$). For PIN1:PIN1-GFP and PIN3:PIN3-GFP, plants were analyzed at 6 to 7 weeks of age. For PIN7:PIN7-GFP, plants were stage matched by comparing plants with inflorescence stems 18 to 20 cm in height. Error bars indicate SE, and the statistical comparisons shown were made between the mutant and the wild type (Student's *t* test, *, $P < 0.05$ and **, $P < 0.01$).

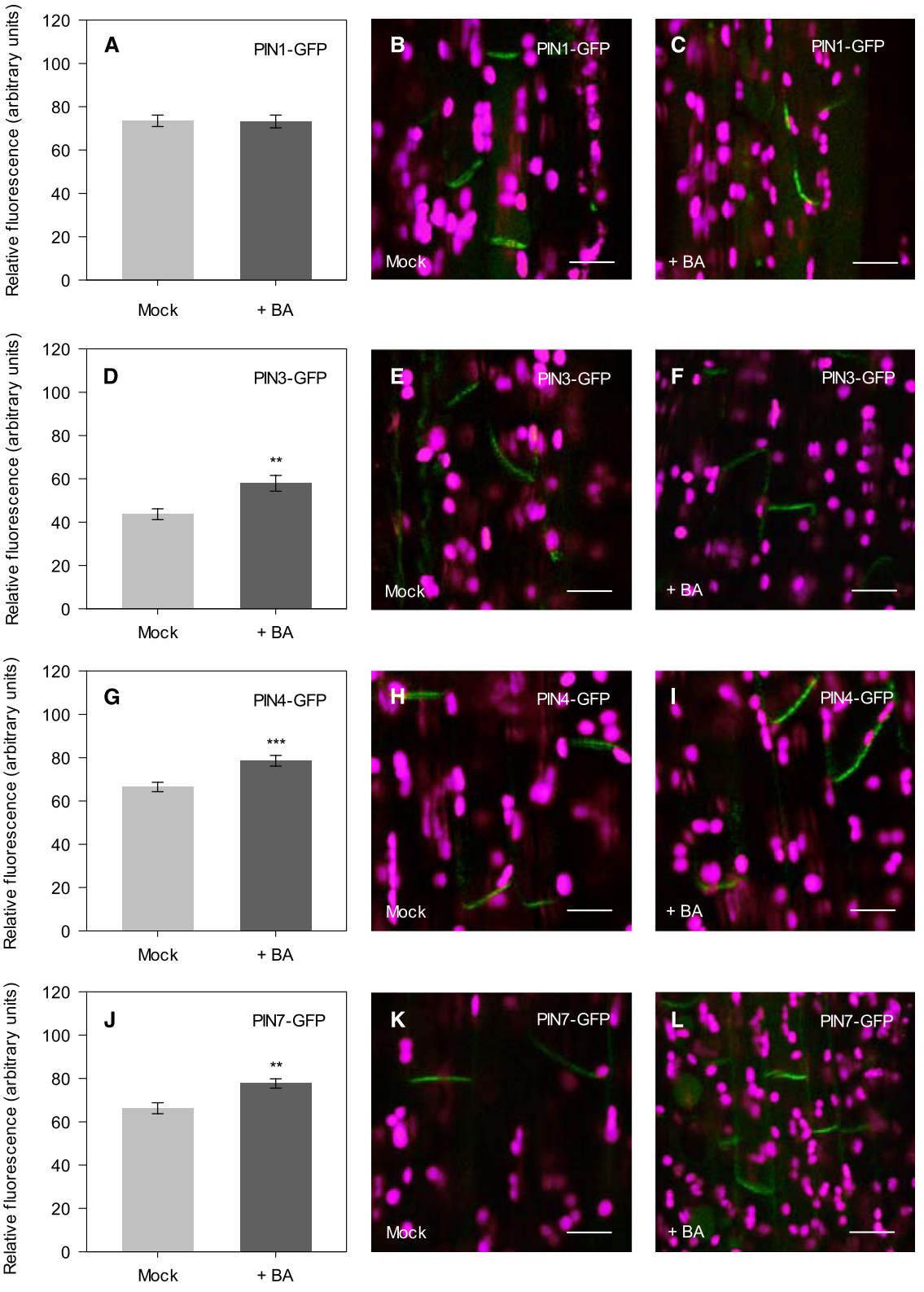

Figure 6. Cytokinin promotes the accumulation of PIN3-GFP, PIN4-GFP, and PIN7-GFP on the basal plasma membrane of xylem parenchyma cells in inflorescence stems. Vertically held basal inflorescence internode segments (~2 cm) from *PIN1:PIN1-GFP* (A–C), *PIN3:PIN3-GFP* (D–F), *PIN4:PIN4-GFP* (G–I), and *PIN7:PIN7-GFP* (J–L) plants (all Col-0 background) were treated apically with 1 μM NAA and basally with either 0.1% DMSO control (Mock) or 1 μM BA (+ BA). After 4 h, stem segments were sectioned longitudinally at their basal ends and imaged using confocal microscopy. The amount of GFP signal on the

amount of PIN1-GFP on the basal plasma membrane was unchanged in mock versus BA-treated stems (Fig. 6, A–C). BA treatment increased the amount of PIN3-GFP on the basal plasma membrane by ~30% ($P < 0.01$; Fig. 6, D–F), PIN4-GFP by ~20% ($P < 0.001$; Fig. 6, G–I), and PIN7-GFP by ~15% ($P < 0.01$; Fig. 6, J–L). No changes in the steady-state transcript levels of *PIN1*, *PIN3*, *PIN4*, or *PIN7* were found in the basal 5 mm of equivalently treated wild-type inflorescence internodes after 4 h of BA treatment (Supplemental Fig. S6). When tracking individual PIN7:PIN7-GFP-expressing xylem parenchyma cells in a longitudinal section for 2 h, the amount of PIN7-GFP on the basal plasma membrane of NAA-treated internodes generally decreased over time, but cells treated with a combination of NAA and BA retained more PIN7-GFP signal compared with cells treated with NAA alone ($P < 0.01$; Supplemental Fig. S7).

Together, these results demonstrate that CK affects plasma membrane levels of PIN3, PIN4, and PIN7 proteins in inflorescence stems, and this correlates with changes in auxin transport. The effect of CK on these PINs may be posttranscriptional, and the response has some specificity, since PIN1 is unaffected.

Nitrate Phenocopies the Effect of CK on PIN Proteins in Stems

Nitrate supply promotes shoot branching in Arabidopsis, but the mechanisms underlying this response are complex, with multiple modes of action likely (de Jong et al., 2014). The response of branching to nitrate is unlikely to involve PIN1, since steady-state PIN1-GFP levels in the stem remain the same under different nitrate regimes (de Jong et al., 2014). It is well established that CK can act as a nitrate signal (Sakakibara et al., 2006), and consistent with this, we previously showed that higher order *ipt3,5,7* and *arr3,4,5,6,7,15* mutants form similar numbers of branches under high- and low-nitrate conditions, suggesting that CK contributes to the ability of Arabidopsis plants to modulate branching in response to nitrate supply (Müller et al., 2015). The CK responsiveness of PIN3, PIN4, and PIN7 suggests a possible route for nitrate-mediated regulation of branching via CK. To assess whether changes in nitrate status might be reflected in PIN3, PIN4, and PIN7 accumulation, PIN3:PIN3-GFP, PIN4:PIN4-GFP, and PIN7:PIN7-GFP plants were grown under nitrate-sufficient and -insufficient conditions, and the amount of PIN-GFP signal on the basal plasma membrane of xylem parenchyma cells was quantified in basal inflorescence internodes. As for exogenous CK supply, nitrate-sufficient conditions were associated with increased levels of PIN3-GFP, PIN4-GFP, and PIN7-GFP on the basal plasma membrane (Fig. 7). Under low-nitrate conditions, PIN3-GFP was reduced to ~75% of the levels observed in high-nitrate plants ($P < 0.001$; Fig. 7A), while PIN4-GFP and PIN7-GFP were reduced to ~85% of that in high-nitrate plants ($P < 0.001$; Fig. 7, B and C). These results are consistent with the idea that nitrate modulates shoot branching at least in part via CK effects on PIN3, PIN4, and PIN7 abundance; however, it is also possible that nitrate supply modulates PIN3, PIN4, and PIN7 accumulation via a CK-independent mechanism.

PIN3, PIN4, and PIN7 Contribute to Shoot-Branching Control in *arr1*

To assess the contribution of changes in PIN3, PIN4, and PIN7 to CK-mediated branching control, we generated the *arr1 pin3 pin4 pin7* quadruple mutant (hereafter referred to as *arr1 pin3,4,7*) and analyzed its branching phenotype. As the differences in branch numbers between the wild type, *arr1*, and *pin3,4,7* are typically small, plants were grown under short days for 4 weeks initially and then shifted to long days for 5 weeks in order to maximize branch numbers, providing sensitized conditions to assess any differences. At terminal flowering, an intermediate number of branches were formed in the *arr1 pin3,4,7* quadruple mutant (9.9) compared with the *arr1* single mutant (12.1) and the *pin3,4,7* triple mutant (8.4; Fig. 8, A–F). This reduction in branching of *arr1* in the *pin3,4,7* mutant background is consistent with the hypothesis that CK-regulated changes in PIN3, PIN4, and PIN7 contribute to the increased shoot-branching phenotype of *arr1*. The *pin3,4,7* mutant exhibits twisted rosette leaves and an increased cauline branch angle phenotype (Bennett et al., 2016), and in both these aspects, the *arr1 pin3,4,7* quadruple mutant appeared similar to the *pin3,4,7* triple mutant (Fig. 8, A–E and G).

To assess the responses of *pin3,4,7* buds to exogenous CK treatment, we used the same experimental setup described for *arr1*, in which buds on isolated nodal stem segments were treated with apical NAA and basal BA supplied through the stem. Overall, the *pin3,4,7* triple mutant responded similarly to the wild type, activating in mock and basal BA treatments and remaining inhibited for several days in the presence of

Figure 6. (*Continued*.)
basal plasma membrane of xylem parenchyma cells was quantified in five cells each from at least seven independent plants for *PIN1:PIN1-GFP* (A), 10 independent plants for *PIN3:PIN3-GFP* (D) and *PIN4:PIN4-GFP* (G), or 11 independent plants for *PIN7:PIN7-GFP* (J). Error bars indicate SE, and the statistical comparisons shown were made between mock- and BA-treated stems (Student's *t* test, **, $P < 0.01$ and ***, $P < 0.001$). Representative confocal images used for GFP quantifications are shown for mock-treated (B, E, H, and K) and BA-treated (C, F, I, and L) stems. Green shows PIN-GFP signal, and magenta shows chloroplast autofluorescence. *PIN1:PIN1-GFP* and *PIN3:PIN3-GFP* plants were analyzed at 5 to 6 weeks of age. *PIN4:PIN4-GFP* and *PIN7:PIN7-GFP* plants were analyzed at 4 to 5 weeks of age and stage matched across treatments according to inflorescence height. Bars = 10 μm.

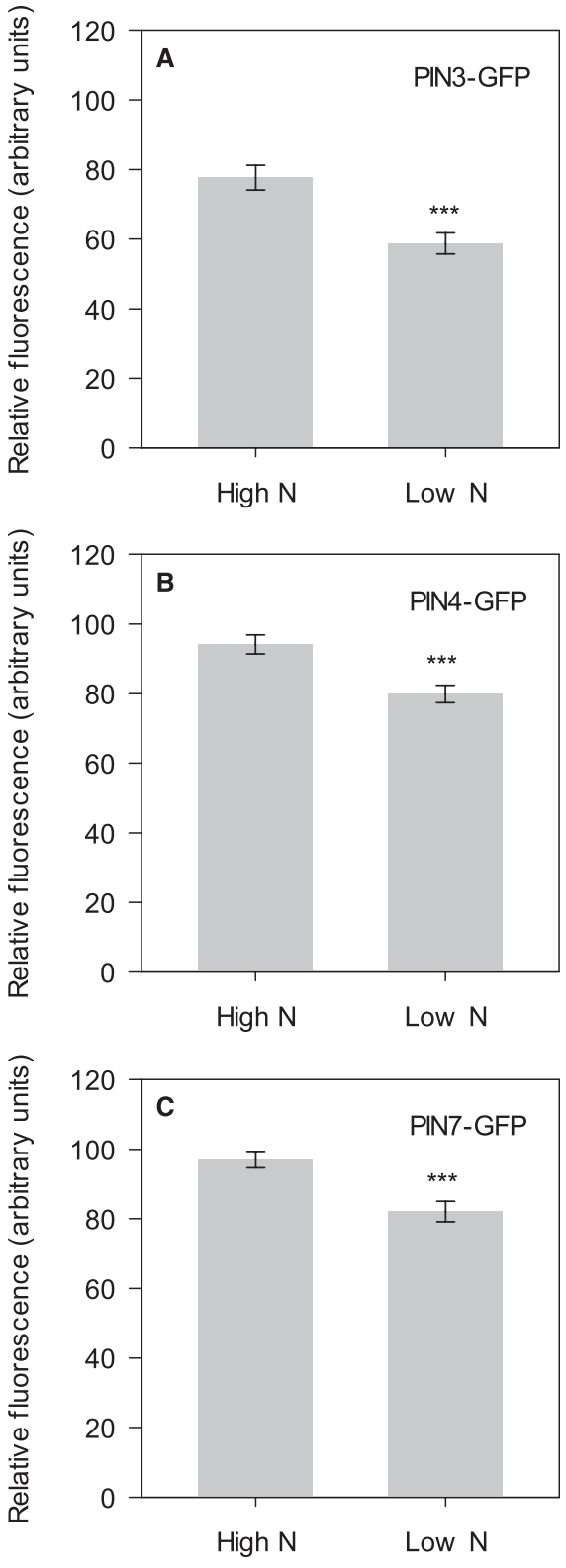

Figure 7. Growth on low-nitrate conditions reduces PIN-GFP accumulation. *PIN3:PIN3-GFP* (A), *PIN4:PIN4-GFP* (B), and *PIN7:PIN7-GFP* (C) plants (all Col-0 background) were grown on a sand and Terra Green mix supplemented with ATS medium containing 9 mM NO_3 (high N) or 1.8 mM NO_3 (low N). Basal inflorescence internodes were sectioned longitudinally and imaged at 4 to 6 weeks of age using confocal microscopy. *PIN7:PIN7-GFP* plants were stage matched based on inflorescence heights across nitrate treatments. The amount of GFP signal on the basal plasma membrane was quantified in the xylem parenchyma using five cells each from eight independent plants for C (n = 40). Error bars indicate SE, and the statistical comparisons shown were made between high- and low-nitrate-treated plants (Student's t test, ***, $P < 0.001$).

apical NAA (Fig. 9, A and B). As for the wild type, basal BA could override the effect of apical NAA in *pin3,4,7* mutants; however, mutant buds activated significantly faster than wild-type buds during the first 4 d (Fig. 9C). Together, the results suggest that PIN3, PIN4, and PIN7 contribute to CK-mediated bud activation, but the phenotypic effects of the *pin3,4,7* mutation suggest that CK also functions via other mechanisms.

DISCUSSION

Perturbing CK levels through exogenous application or through the manipulation of endogenous levels provides clear evidence that CK can promote bud activation (Wickson and Thimann, 1958; Faiss et al., 1997; Chatfield et al., 2000; Müller et al., 2015). Elucidating the role of the known CK signaling pathway in bud activation has been less straightforward, due to the large gene families involved and consequent functional redundancy. Previously, we showed that the *arr3,4,5,6,7,15* mutant has reduced branching and its buds are CK resistant, an unexpected result, since type-A ARRs are generally considered to be negative regulators of CK signaling (Müller et al., 2015). Since the type-A ARRs are themselves transcriptionally induced by CK as part of a negative feedback loop, loss-of-function mutations in these genes could have complex phenotypes with respect to the CK response. However, our demonstration that the *arr1* mutant has a branching phenotype opposite to *arr3,4,5,6,7,15* suggests that the type-A and type-B ARRs do indeed function antagonistically in bud activation, leaving the paradox unresolved.

ARR1- and *ARR3,4,5,6,7,15*-Independent CK Signaling and Shoot Branching

ARR1 is a well-characterized positive regulator of CK signaling and regulates the expression of CK-responsive genes (Sakai et al., 2001). Throughout our analyses of shoot branching and associated auxin transport phenotypes, *arr1* phenocopied CK treatment, whereas *arr3,4,5,6,7,15* phenocopied CK depletion, as in *ipt3* (Figs. 1 and 3–6; Supplemental Figs. S2 and S4). This raises the interesting prospect that the *arr* mutant phenotypes are due to feedback regulation of the pool of active CKs via synthesis or degradation, such that reduced CK signaling in *arr1* leads to an increase in the pool of active CKs, while increased CK signaling in *arr3,4,5,6,7,15* reduces the pool of active CKs. Such

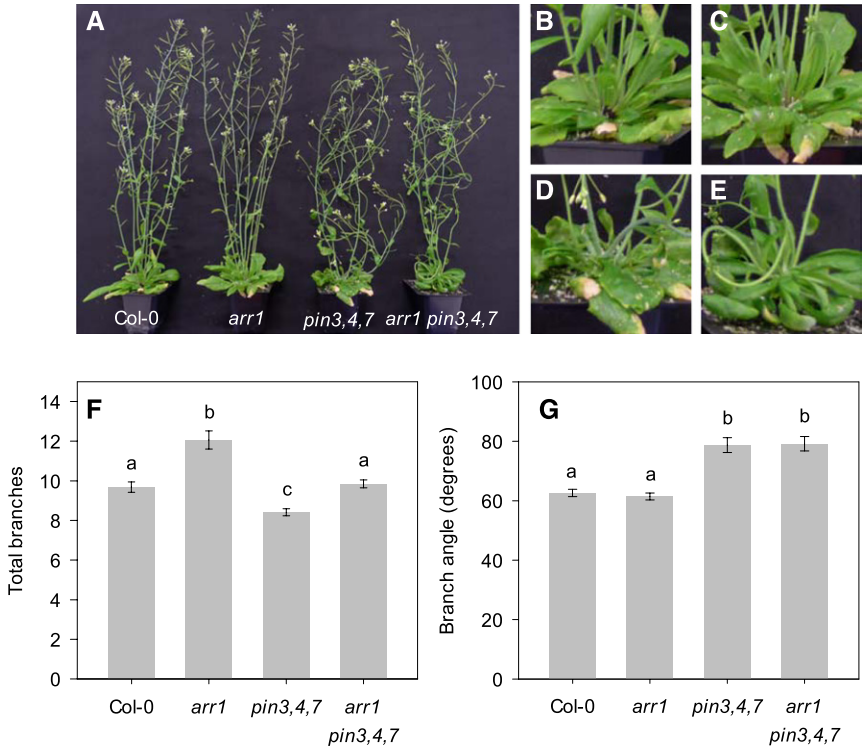

Figure 8. Interactions between *arr1* and *pin3,4,7* in shoot-branching control. A to E, Shoot phenotypes of ~6-week-old Col-0, *arr1*, *pin3,4,7*, and *arr1 pin3,4,7* plants grown under long days. Closeup views of the rosettes in A are shown in B (Col-0), C (*arr1*), D (*pin3,4,7*), and E (*arr1 pin3,4,7*). F, Total number of branches formed at terminal flowering on ~9-week-old wild-type, *arr1*, *pin3,4,7*, and *arr1 pin3,4,7* plants grown under short days for 4 weeks and then long days for 5 weeks (n = 16–47). Error bars indicate SE. Letters denote significant differences between genotypes (Kruskal-Wallis H test, $P < 0.05$). G, Angles between the emergence point of branches on the primary inflorescence in wild-type, *arr1*, *pin3,4,7*, and *arr1 pin3,4,7* plants at ~6 weeks of age. Two cauline branches were analyzed per plant from at least 13 independent plants (n = 26–46). Error bars indicate SE. Letters denote significant differences (ANOVA, Tukey's b posthoc test, $P < 0.05$).

feedback between hormone signaling and hormone levels is well established for most plant hormones, including CK. For example, CK application induces the expression of genes encoding CYTOKININ OXIDASE-degrading enzymes (Kiba et al., 2002; Rashotte et al., 2003), and this also has been observed in CK-treated buds (Müller et al., 2015). Consistent with this feedback, the triple *ahk2 ahk3 cre1* CK receptor mutant has elevated levels of N^6-(Δ2-isopentenyl)-adenine precursor and trans-zeatin-type CKs in young plants (Riefler et al., 2006). This feedback has the potential to account for the high-CK increased branching phenotype of the *arr1* mutant and the low-CK reduced branching phenotype of the *arr3,4,5,6,7,15* mutant (Fig. 10).

Importantly, in addition to shoot branching, the phenotypic correlations we observe in *arr* mutants extend to auxin transport properties. CK treatment, nitrate supply, and loss of *ARR1* result in the overaccumulation of PIN3, PIN4, and PIN7, whereas CK-depleting conditions, such as *ipt3* mutation or nitrate starvation, and loss of the *ARR3,4,5,6,7,15* clade result in PIN3, PIN4, and PIN7 depletion. If CK homeostasis is indeed altered in the *arr* mutants, this implies that CK can signal independently of the ARR genes analyzed here to promote PIN3, PIN4, and PIN7 accumulation (Fig. 10). One possibility is that CK can signal entirely independently of ARRs via a noncanonical pathway or simply independently of *ARR1* and *ARR3,4,5,6,7,15*, for example, through a specialized type-B family member (or members) via the canonical pathway. Further work will be required to understand precisely which CK signaling components target PIN proteins in shoots. No differences were observed in PIN1 accumulation, suggesting that specific auxin transporters are targeted by this signaling route.

The lack of change in *PIN* gene expression levels in type-A and type-B *arr* mutants and in wild-type plants in response to CK addition suggests that *PIN* transcription is not a direct target for CK signaling in bud activation, by whatever pathway, and suggests that the effect of CK on PINs is posttranscriptional (Supplemental Figs. S3 and S6). This could be a protein-level effect on PINs, similar to that established for SLs and PIN1, or it could be a transcriptional effect on PIN regulators. For example, PINOID-dependent (PID) phosphorylation can modulate the apical-basal polarity of PINs (Friml et al., 2004), and *PID* gene expression is reduced in shoots within 2 h of CK treatment in

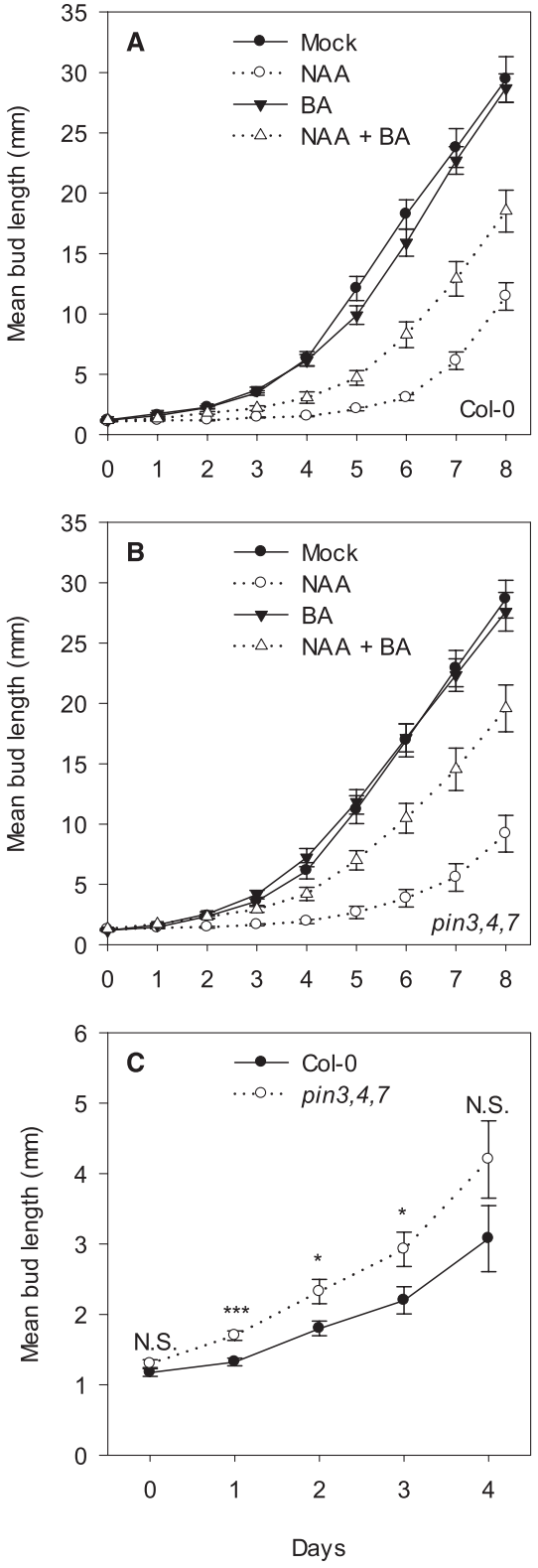

Figure 9. *pin3,4,7* exhibits altered bud activation in response to BA. A and B, Bud length of wild-type Col-0 (A) and *pin3,4,7* (B) isolated nodal segments treated for 8 d with mock, 1 μM NAA (apical), 1 μM BA (basal), or combined 1 μM NAA (apical) and 1 μM BA (basal; $n = 19–20$ per treatment). C, Closeup of days 0 to 4 for wild-type and *pin3,4,7* buds treated with combined apical NAA and basal BA. Error bars indicate SE. N.S. denotes no significant difference between treatments. Asterisks denote statistically significant differences between treatments (Student's *t* test, *, $P < 0.05$ and ***, $P < 0.001$).

Arabidopsis seedlings, consistent with CK promoting basal localization of PINs (Brenner and Schmülling, 2012). Such a posttranscriptional effect on PINs acting via the canonical CK signaling pathway has been established in roots. In the octuple *arr3,4,5,6,7,8,9,15* mutant, lower levels of GFP-tagged translational fusions of *PIN1*, *PIN3*, and *PIN4* are observed in root tips, whereas *PIN7* is reduced in the stele but increased in the root cap, and these changes do not correlate with *PIN* transcript abundances (Zhang et al., 2011). In contrast to our results, this effect mirrors CK treatment, as expected if the type-A ARRs are acting as negative regulators of CK signaling.

The Role of the Auxin Transport System in the Regulation of Shoot Branching by CK

Our results show a strong correlation between CK, the basal membrane abundance of PIN3, PIN4, and PIN7, bulk auxin transport, and shoot branching across all our experiments. Reducing auxin transport with the pharmacological inhibitor NPA has opposite effects on branching in *arr1* and *arr3,4,5,6,7,15* (Fig. 3), suggesting a causal link between auxin transport perturbation and the *arr* mutant shoot-branching phenotypes. The *pin3,4,7* triple mutant partially suppresses the increased branching of *arr1* mutants, consistent with the idea that this phenotype is caused in part by overaccumulation of these PINs (Bennett et al., 2016; Fig. 8). One explanation for this relationship is that CK-mediated increases in PIN3, PIN4, and PIN7 accumulation increase the initial flow of auxin between the bud and the PATS, thereby supporting the establishment of canalized auxin transport between the bud and the stem and increasing the ease with which buds can activate. Consistent with this idea, polarized PIN1 protein can be observed at the bud-stem junction in pea within 24 h of CK treatment (Kalousek et al., 2010) and CK applied to axillary buds can promote the export of auxin out of the buds (Li and Bangerth, 2003). This hypothesis is also consistent with the resistance of *arr1* buds to the inhibitory effects of the SL analogue GR24 (Fig. 2). SL acts in part by dampening the positive feedback in auxin transport canalization between the bud and the stems. Increased PIN3-, PIN4-, and PIN7-mediated bud-stem auxin flux could counteract SL-mediated PIN1 removal by promoting additional flux-correlated PIN1 allocation. According to this model, it is the role of PIN3, PIN4, and PIN7 in cross-stem auxin flux, rather than basipetal transport down the stem, that is important in CK-mediated bud activation. This is consistent with our previous analyses demonstrating that PIN3, PIN4, and PIN7 play an important role in the ability of consecutive buds on opposite sides of the

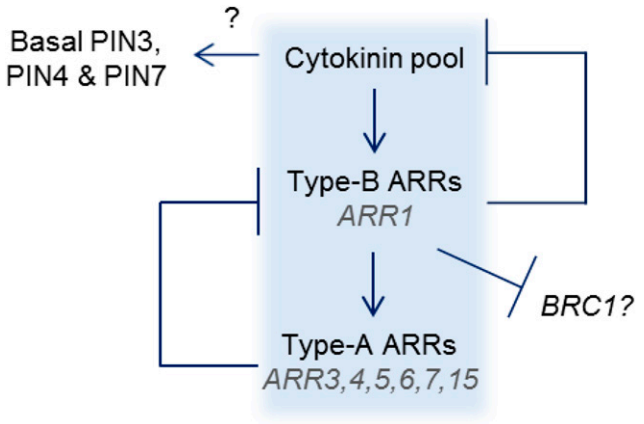

Figure 10. Proposed model for CK signaling in bud outgrowth regulation. Canonical CK signaling via the type-B ARR1 results in feedback-mediated down-regulation of CK levels as part of signal perception. Members of the type-A ARR family are transcriptionally induced by ARR1 and/or other type-B family members and dampen type-B-mediated signaling, including the feedback-mediated down-regulation of CK levels. The basal plasma membrane accumulation of PIN3, PIN4, and PIN7 in xylem parenchyma cells in the main stem is enhanced by CK by an unknown mechanism. In parallel, the expression of other bud regulatory genes such as *BRC1* may be targeted by the canonical CK signaling pathway.

stem to inhibit one another's outgrowth while having only limited impact on the total level of shoot branching in intact plants.

Importantly, the *pin3,4,7* mutant only partially suppresses the *arr1* shoot-branching phenotype, and *pin3,4,7* buds respond strongly to basal BA supply in isolated nodal assays, even activating slightly earlier than wild-type buds when treated with a combination of apical NAA and basal BA. These results demonstrate that CK can activate buds through PIN3-, PIN4-, and PIN7-independent mechanisms. The mechanism(s) underlying faster *pin3,4,7* bud activation in response to apical NAA and basal BA is not known. In Arabidopsis, the ability of SL to inhibit bud activity appears to depend jointly on its ability to promote the accumulation of transcripts of the *BRC1* gene and to trigger endocytosis of PIN1, reducing the ability of buds to establish canalized auxin export into the stem. Our data for CK support a similar dual activity for CK, reducing *BRC1* transcript abundance and increasing PIN3, PIN4, and PIN7 accumulation at the plasma membrane (Seale et al., 2017; Fig. 6). One highly speculative possibility is that the combination of low *BRC1* expression and reduced peripheral stem auxin in *pin3,4,7* mutants might allow for rapid early expansion of the bud.

Other Targets for CK Signaling in Shoot Branching

Our data suggest that CK promotes shoot branching in part by driving plasma membrane accumulation of PIN3, PIN4, and PIN7. This would operate in parallel with the established ability of CK to regulate transcription in buds, for example, by down-regulating expression of the *BRC1* bud regulatory gene (Fig. 10; Aguilar-Martínez et al., 2007; Poza-Carrión et al., 2007; Braun et al., 2012; Dun et al., 2012; Seale et al., 2017). The parallel operation of these two mechanisms makes interpretation of the *arr* mutant phenotypes complicated. For example, in the *arr1* mutant, impaired CK-induced changes in transcription should lead to reduced shoot branching. Consistent with this, the *arr1* mutant has reduced steady-state type-A *ARR* gene expression, as expected if there is reduced CK signaling via the canonical pathway (Supplemental Fig. S8). At the same time, it is possible that this results in the overaccumulation of CK due to impaired feedback regulation of CK levels. This CK could signal in an *ARR1*-independent manner to promote PIN3, PIN4, and PIN7 accumulation, thereby promoting shoot branching. Thus, it is likely that the *arr1* shoot-branching phenotype is a compromise between these opposing effects. Added to this, there is likely to be some redundancy in the type-B ARR family, and it is possible that different family members are differentially important in regulating feedback on CK synthesis versus modulation of the transcription of bud-regulating genes. Given all these considerations, there are many alternative ways to interpret our result that *arr1* mutant buds inhibited by apical NAA supply can be activated by basal BA similar to the wild type, whereas *arr3,4,5,6,7,15* buds cannot (Müller et al., 2015).

CONCLUSION

Several studies have proposed a causal link between CK and increased auxin transport as one mechanism for CK-mediated bud outgrowth (Davies et al., 1966; Chatfield et al., 2000; Li and Bangerth, 2003). Our results support this hypothesis, and in particular, we demonstrate that CK drives the accumulation of PIN3, PIN4, and PIN7 on the plasma membrane, and this contributes to the branching phenotype observed in the *arr1* mutant. Interestingly, the phenotypes of type-A and type-B *arr* CK signaling mutants are the opposite of those expected given their respective negative and positive roles in CK-mediated transcriptional control in roots. This suggests a strong specialization within the ARR gene families or an ARR-independent mechanism for CK signaling in the control of shoot branching.

MATERIALS AND METHODS

Plant Lines

Arabidopsis (*Arabidopsis thaliana*) Col-0 was used as the wild type for all experiments. The *arr3,4,5,6,7,15* line was published previously (Müller et al., 2015). The homozygous *arr1-4* (SALK_042196) T-DNA insertion line was obtained from the Nottingham Arabidopsis Stock Centre and identified using ARR1-4 LP (5′-GATCAAACCCATTCAATGTCG-3′), ARR1-4 RP (5′-GAGATGGCATTGTCTCTGCTC-3′), and LBb1.3 according to the SALK T-DNA Web site (http://signal.salk.edu/tdnaprimers.2.html) (www.signal.salk.edu/

tdnaprimers.2.html; Alonso et al., 2003). The *PIN1:PIN1-GFP* (Benková et al., 2003), *PIN3:PIN3-GFP* (Zádníková et al., 2010), *PIN4:PIN4-GFP* (Bennett et al., 2016), and *PIN7:PIN7-GFP* (Blilou et al., 2005) reporter lines have been described previously. All *PIN:PIN-GFP* reporter lines on the *arr3,4,5,6,7,15* mutant background were generated by crossing *arr3,4,5,6,7,15* to each of the *arr3,4,5,6,7,8,9,15* PIN-GFP lines described previously (Zhang et al., 2011) and screened for the presence of wild-type *ARR8* (forward, 5′-CAAATGGCTGTTAAAACCCACCAATA-3′; and reverse, 5′-CCATTGTTAGTGTGCTATCACCTGAGTG-3′) and *ARR9* (forward, 5′-CAGACTCTTTATTTCTCTTCCTC-3′; and reverse, 5′-CCCACATACAACATCATCATCATATTCC-3′) genes. For *arr1*, the four Col-0 PIN:PIN-GFP lines were crossed to *arr1-4*. Segregants were screened in the F2 and F3 generations for GFP and the correct genotype using the above gene-specific primers and *ARR3*, *ARR4*, *ARR5*, *ARR6*, *ARR7*, and *ARR15* primers published previously (To et al., 2004; Zhang et al., 2011).

Growth Conditions

Seeds were stratified for 3 to 5 d at 4°C. Soil-grown plants were sown onto F2 soil treated with Intercept 70WG (both Levington) or Exemptor (ICL) in PT24 or PT40 trays in controlled environment rooms under long-day (16 h of light/8 h of dark) or short-day (8 h of light/16 h of dark) photoperiods. For plants grown under sterile conditions, seeds were vapor sterilized with 100 mL of 10% (w/v) chlorine bleach and 3 mL of 10.2 M HCl for 4 h and sown onto solidified ATS medium (containing 0.8% [w/v] agar; Wilson et al., 1990). Soil- and sterile-grown plants were subject to an average light intensity of 170 or 100 µmol m^{-2} s^{-1}, respectively, and an average temperature range of 17°C to 21°C.

Branch Counts

Primary rosette and cauline branches of 1 cm or more were counted on intact plants at or near terminal flowering. Decapitation assays were performed according to Greb et al. (2003).

Hormone and NPA Treatments

For testing bud responses to NAA, BA, and GR24, plants were grown under sterile conditions and one-node assays were performed as described previously (Chatfield et al., 2000; Müller et al., 2015). For treating whole plants with NPA or GR24, plants were grown for 6 weeks under sterile conditions on solidified ATS medium in glass jars as described previously (Bennett et al., 2006; Crawford et al., 2010). For NAA and BA treatment of stems, 2 cm segments from the basal inflorescence internode were collected from soil-grown plants. Similar to the one-node assay system, segments were placed vertically onto split plates prepared with 1 µM NAA in the upper apical portion and either mock (DMSO) or 1 µM BA in the lower basal portion or the apical portion. Plates were prepared by cutting a 1 cm trough through the middle of square 10 cm plates containing 50 mL of solidified ATS medium without Suc. Hormone or mock solutions were pipetted into the upper or lower half (25 µL of 1,000× stocks). Plates were placed under standard light conditions for sterile-grown plants.

Reverse Transcription-Quantitative PCR

For analysis of *PIN1*, *PIN3*, *PIN4*, and *PIN7* gene expression levels in the *arr1* and *arr3,4,5,6,7,15* mutants, seeds were sown in glass jars on solidified ATS medium as described above for whole-plant NPA and GR24 treatments. Plants were grown for 6 weeks, and the uppermost inflorescence internodes (i.e. the inflorescence stem between the uppermost two cauline nodes) were harvested onto liquid nitrogen. Three biological replicates each containing 10 to 15 internodes were collected. For NAA and BA treatments, 2 cm segments from the basal inflorescence internodes were collected from 6 week-old soil-grown plants and placed vertically onto plates containing apical NAA with or without basal BA, prepared as above. Treatments were left for 4 h, and the basal 5 mm of the 2 cm segments was harvested into three biological replicates of six to seven segments each on liquid nitrogen. RNA extractions, cDNA synthesis, and quantification of transcript levels were carried out as described previously (Müller et al., 2015) using 650 or 500 ng of total RNA for the *arr* or BA response analysis, respectively. Sequences of the primers used are as follows: *PIN1* forward, 5′-CAGTCTTGGGTTGTTCATGGC-3′; *PIN1* reverse, 5′-ATCTCATAGCCGCCGCAAAA-3′; *PIN3* forward, 5′-CCATGGCGGTTAGGTTCCTT-3′; *PIN3* reverse, 5′-ATGCGGCCTGAACTATAGCG-3′; *PIN4* forward, 5′-AATGCTAGAGGTGGTGGTGATG-3′; *PIN4* reverse, 5′-TAGCTCCGCCGTGGAATTAG-3′; *PIN7* forward, 5′-GGTGAAAACAAAGCTGGTCCG-3′; and *PIN7* reverse, 5′-CCGAAGCTTGTGTAGTCCGT-3′. For Supplemental Figure S8, *ARR1* forward, 5′-TACGAAGTAACGAAATGCAACAGA-3′; *ARR1* reverse, 5′-GAAACCGTCCATGTCAGGCA-3′; and previously published primer sequences for *ARR4*, *ARR5*, *ARR6*, *ARR7*, and *ARR15* were used (Müller et al., 2015).

Microscopy

For *PIN1:PIN1-GFP* and *PIN3:PIN3-GFP*, which exhibit relatively stable levels of expression in the stem throughout development, basal inflorescence internodes from ~6-week-old soil-grown plants were collected for imaging. For *PIN4:PIN4-GFP* and *PIN7:PIN7-GFP*, which exhibit reductions in stem expression during development, inflorescence internodes were taken from 4 to 5 week-old soil-grown plants when the inflorescence was ~5 to 15 cm high. Between treatments, individual plants were stage matched so that the same internodes from two plants with inflorescence heights within 1 cm of each other were compared. Internodes were hand sectioned longitudinally through vascular bundles using a razor blade and a dissecting microscope, or transversely in 2 mm segments, then secured to a petri dish with micropore tape or embedded in solidified ATS medium and covered in water. Confocal microscopy was performed using a Zeiss LSM700 imaging system with 20× or 10× water-immersion lenses. For longitudinal sections, xylem parenchyma tissues were located by focusing on the spiral pattern of xylem cell wall lignin under transmitted light. Excitation was performed using 488 nm (3%–6% laser power) and 639 nm (2% laser power) lasers. Images were acquired using SP555 and LP640 emission filters for GFP and chloroplast autofluorescence, respectively. The same detection settings were used within an experiment. For longitudinal sections, GFP fluorescence intensities were quantified by manually tracing around the basal plasma membrane of a nonsaturated cell using Zeiss ZEN 2012 software. At least five cells each from eight to 10 individual plants were analyzed per treatment and repeated at least once. For transverse sections, Z-stacks were acquired using a 3 to 5 µm step size. Maximum projections generated using ImageJ software and GFP fluorescence (as arbitrary units per pixel) were quantified by manually tracing around vascular bundles. Five vascular bundles were analyzed from at least five individual plants and repeated at least once. For representative images, projections were made using LSM Image Browser software version 4.2.0.121 and processed in Adobe Photoshop.

Auxin Transport Assays

Auxin transport assays were performed as described by Bennett et al. (2016).

Branch Angle Measurements

Inflorescence stems bearing two branches from mature plants were trimmed, laid flat, and photographed. The angle between the point of emergence and the inflorescence stem was measured using ImageJ software.

Statistical Analyses

Statistical analyses were performed using SPSS Statistics version 22.

Accession Numbers

Sequence data from this article can be found on TAIR (www.arabidopsis.org) under accession numbers AT3G16857 (ARR1), AT1G59940 (ARR3), AT1G10470 (ARR4), AT3G48100 (ARR5), AT5G62920 (ARR6), AT1G19050 (ARR7), AT1G74890 (ARR15), AT3G63110 (IPT3), AT1G73590 (PIN1), AT1G70940 (PIN3), AT2G01420 (PIN4), and AT1G23080 (PIN7).

Supplemental Data

The following supplemental materials are available.

Supplemental Figure S1. GR24 dose response of the wild type and *arr1*.

Supplemental Figure S2. *ipt3* has reduced stem auxin transport.

Supplemental Figure S3. *PIN* gene expression in the wild type and *arr1* and *arr3,4,5,6,7,15* mutants.

Supplemental Figure S4. PIN7-GFP is reduced in *ipt3* inflorescence stems.

Supplemental Figure S5. PIN7-GFP expression in *arr1* inflorescence stems over time.

Supplemental Figure S6. *PIN* gene expression is unchanged in inflorescence stems after 4 h of BA treatment.

Supplemental Figure S7. BA promotes the accumulation of PIN7:PIN7-GFP on the basal plasma membrane of xylem parenchyma cells within 2 h.

Supplemental Figure S8. Expression of *ARR* genes in *arr* mutants.

ACKNOWLEDGMENTS

We thank Joseph Kieber for supplying the *arr3,4,5,6,7,8,9,15* PIN-GFP reporter lines, Ruth Stephens for excellent technical assistance, and Tom Bennett and Martin van Rongen for helpful advice and discussions.

Received November 22, 2017; accepted April 23, 2018; published May 1, 2018.

LITERATURE CITED

Aguilar-Martínez JA, Poza-Carrión C, Cubas P (2007) *Arabidopsis BRANCHED1* acts as an integrator of branching signals within axillary buds. Plant Cell **19**: 458–472

Alonso JM, Stepanova AN, Leisse TJ, Kim CJ, Chen H, Shinn P, Stevenson DK, Zimmerman J, Barajas P, Cheuk R, (2003) Genome-wide insertional mutagenesis of Arabidopsis thaliana. Science **301**: 653–657

Bainbridge K, Sorefan K, Ward S, Leyser O (2005) Hormonally controlled expression of the Arabidopsis *MAX4* shoot branching regulatory gene. Plant J **44**: 569–580

Bangerth F (1994) Response of cytokinin concentration in the xylem exudate of bean (*Phaseolus vulgaris* L.) plants to decapitation and auxin treatment, and relationship to apical dominance. Planta **194**: 4

Benková E, Michniewicz M, Sauer M, Teichmann T, Seifertová D, Jürgens G, Friml J (2003) Local, efflux-dependent auxin gradients as a common module for plant organ formation. Cell **115**: 591–602

Bennett T, Sieberer T, Willett B, Booker J, Luschnig C, Leyser O (2006) The *Arabidopsis MAX* pathway controls shoot branching by regulating auxin transport. Curr Biol **16**: 553–563

Bennett T, Hines G, van Rongen M, Waldie T, Sawchuk MG, Scarpella E, Ljung K, Leyser O (2016) Connective auxin transport in the shoot facilitates communication between shoot apices. PLoS Biol **14**: e1002446

Blilou I, Xu J, Wildwater M, Willemsen V, Paponov I, Friml J, Heidstra R, Aida M, Palme K, Scheres B (2005) The PIN auxin efflux facilitator network controls growth and patterning in *Arabidopsis* roots. Nature **433**: 39–44

Booker J, Chatfield S, Leyser O (2003) Auxin acts in xylem-associated or medullary cells to mediate apical dominance. Plant Cell **15**: 495–507

Braun N, de Saint Germain A, Pillot JP, Boutet-Mercey S, Dalmais M, Antoniadi I, Li X, Maia-Grondard A, Le Signor C, Bouteiller N, (2012) The pea TCP transcription factor PsBRC1 acts downstream of strigolactones to control shoot branching. Plant Physiol **158**: 225–238

Brenner WG, Schmülling T (2012) Transcript profiling of cytokinin action in Arabidopsis roots and shoots discovers largely similar but also organ-specific responses. BMC Plant Biol **12**: 112

Chatfield SP, Stirnberg P, Forde BG, Leyser O (2000) The hormonal regulation of axillary bud growth in *Arabidopsis*. Plant J **24**: 159–169

Crawford S, Shinohara N, Sieberer T, Williamson L, George G, Hepworth J, Müller D, Domagalska MA, Leyser O (2010) Strigolactones enhance competition between shoot branches by dampening auxin transport. Development **137**: 2905–2913

Davies CR, Seth AK, Wareing PF (1966) Auxin and kinetin interaction in apical dominance. Science **151**: 468–469

de Jong M, George G, Ongaro V, Williamson L, Willetts B, Ljung K, McCulloch H, Leyser O (2014) Auxin and strigolactone signaling are required for modulation of Arabidopsis shoot branching by nitrogen supply. Plant Physiol **166**: 384–395

Domagalska MA, Leyser O (2011) Signal integration in the control of shoot branching. Nat Rev Mol Cell Biol **12**: 211–221

Dun EA, de Saint Germain A, Rameau C, Beveridge CA (2012) Antagonistic action of strigolactone and cytokinin in bud outgrowth control. Plant Physiol **158**: 487–498

Faiss M, Zalubìlová J, Strnad M, Schmülling T (1997) Conditional transgenic expression of the ipt gene indicates a function for cytokinins in paracrine signaling in whole tobacco plants. Plant J **12**: 401–415

Foo E, Turnbull CG, Beveridge CA (2001) Long-distance signaling and the control of branching in the *rms1* mutant of pea. Plant Physiol **126**: 203–209

Foo E, Bullier E, Goussot M, Foucher F, Rameau C, Beveridge CA (2005) The branching gene *RAMOSUS1* mediates interactions among two novel signals and auxin in pea. Plant Cell **17**: 464–474

Friml J, Yang X, Michniewicz M, Weijers D, Quint A, Tietz O, Benjamins R, Ouwerkerk PB, Ljung K, Sandberg G, (2004) A PINOID-dependent binary switch in apical-basal PIN polar targeting directs auxin efflux. Science **306**: 862–865

Geldner N, Anders N, Wolters H, Keicher J, Kornberger W, Muller P, Delbarre A, Ueda T, Nakano A, Jürgens G (2003) The Arabidopsis GNOM ARF-GEF mediates endosomal recycling, auxin transport, and auxin-dependent plant growth. Cell **112**: 219–230

Greb T, Clarenz O, Schäfer E, Müller D, Herrero R, Schmitz G, Theres K (2003) Molecular analysis of the *LATERAL SUPPRESSOR* gene in *Arabidopsis* reveals a conserved control mechanism for axillary meristem formation. Genes Dev **17**: 1175–1187

Hall SM, Hillman JR (1975) Correlative inhibition of lateral bud growth in *Phaseolus vulgaris* L. timing of bud growth following decapitation. Planta **123**: 137–143

Hayward A, Stirnberg P, Beveridge C, Leyser O (2009) Interactions between auxin and strigolactone in shoot branching control. Plant Physiol **151**: 400–412

Johnson X, Brcich T, Dun EA, Goussot M, Haurogné K, Beveridge CA, Rameau C (2006) Branching genes are conserved across species: genes controlling a novel signal in pea are coregulated by other long-distance signals. Plant Physiol **142**: 1014–1026

Kalousek P, Buchtová D, Balla J, Reinöhl V, Procházka S (2010) Cytokinins and polar transport of auxin in axillary pea buds. Acta Univ Agric Silvic Mendel Brun **58**: 10

Kiba T, Yamada H, Mizuno T (2002) Characterization of the ARR15 and ARR16 response regulators with special reference to the cytokinin signaling pathway mediated by the AHK4 histidine kinase in roots of *Arabidopsis thaliana*. Plant Cell Physiol **43**: 1059–1066

Li C, Bangerth F (2003) Stimulatory effect of cytokinins and interaction with IAA on the release of lateral buds of pea plants from apical dominance. J Plant Physiol **160**: 1059–1063

Ljung K, Bhalerao RP, Sandberg G (2001) Sites and homeostatic control of auxin biosynthesis in *Arabidopsis* during vegetative growth. Plant J **28**: 465–474

Miyawaki K, Tarkowski P, Matsumoto-Kitano M, Kato T, Sato S, Tarkowska D, Tabata S, Sandberg G, Kakimoto T (2006) Roles of *Arabidopsis* ATP/ADP isopentenyltransferases and tRNA isopentenyltransferases in cytokinin biosynthesis. Proc Natl Acad Sci USA **103**: 16598–16603

Morris DA (1977) Transport of exogenous auxin in two-branched dwarf pea seedlings (*Pisum sativum* L.): some implications for polarity and apical dominance. Planta **136**: 91–96

Müller D, Waldie T, Miyawaki K, To JP, Melnyk CW, Kieber JJ, Kakimoto T, Leyser O (2015) Cytokinin is required for escape but not release from auxin mediated apical dominance. Plant J **82**: 874–886

Poza-Carrión C, Aguilar-Martínez JA, Cubas P (2007) Role of TCP gene BRANCHED1 in the control of shoot branching in Arabidopsis. Plant Signal Behav **2**: 551–552

Prusinkiewicz P, Crawford S, Smith RS, Ljung K, Bennett T, Ongaro V, Leyser O (2009) Control of bud activation by an auxin transport switch. Proc Natl Acad Sci USA **106**: 17431–17436

Rashotte AM, Carson SD, To JP, Kieber JJ (2003) Expression profiling of cytokinin action in Arabidopsis. Plant Physiol **132**: 1998–2011

Riefler M, Novak O, Strnad M, Schmülling T (2006) *Arabidopsis* cytokinin receptor mutants reveal functions in shoot growth, leaf senescence, seed

size, germination, root development, and cytokinin metabolism. Plant Cell **18**: 40–54

Ruegger M, Dewey E, Hobbie L, Brown D, Bernasconi P, Turner J, Muday G, Estelle M (1997) Reduced naphthylphthalamic acid binding in the *tir3* mutant of *Arabidopsis* is associated with a reduction in polar auxin transport and diverse morphological defects. Plant Cell **9**: 745–757

Sachs T (1981) The control of the patterned differentiation of vascular tissues. Adv Bot Res **9**: 151–262

Sakai H, Honma T, Aoyama T, Sato S, Kato T, Tabata S, Oka A (2001) ARR1, a transcription factor for genes immediately responsive to cytokinins. Science **294**: 1519–1521

Sakakibara H, Takei K, Hirose N (2006) Interactions between nitrogen and cytokinin in the regulation of metabolism and development. Trends Plant Sci **11**: 440–448

Schaller GE, Bishopp A, Kieber JJ (2015) The yin-yang of hormones: cytokinin and auxin interactions in plant development. Plant Cell **27**: 44–63

Seale M, Bennett T, Leyser O (2017) *BRC1* expression regulates bud activation potential but is not necessary or sufficient for bud growth inhibition in *Arabidopsis*. Development **144**: 1661–1673

Shinohara N, Taylor C, Leyser O (2013) Strigolactone can promote or inhibit shoot branching by triggering rapid depletion of the auxin efflux protein PIN1 from the plasma membrane. PLoS Biol **11**: e1001474

Tanaka M, Takei K, Kojima M, Sakakibara H, Mori H (2006) Auxin controls local cytokinin biosynthesis in the nodal stem in apical dominance. Plant J **45**: 1028–1036

Teichmann T, Muhr M (2015) Shaping plant architecture. Front Plant Sci **6**: 233

Thimann KV, Skoog F (1933) Studies on the growth hormone of plants. III. The inhibiting action of the growth substance on bud development. Proc Natl Acad Sci USA **19**: 714–716

To JP, Haberer G, Ferreira FJ, Deruère J, Mason MG, Schaller GE, Alonso JM, Ecker JR, Kieber JJ (2004) Type-A *Arabidopsis* response regulators are partially redundant negative regulators of cytokinin signaling. Plant Cell **16**: 658–671

Wickson M, Thimann KV (1958) The antagonism of auxin and kinetin in apical dominance. Physiol Plant **11**: 62–74

Wilson AK, Pickett FB, Turner JC, Estelle M (1990) A dominant mutation in *Arabidopsis* confers resistance to auxin, ethylene and abscisic acid. Mol Gen Genet **222**: 377–383

Zádníková P, Petrásek J, Marhavý P, Raz V, Vandenbussche F, Ding Z, Schwarzerová K, Morita MT, Tasaka M, Hejátko J, (2010) Role of PIN-mediated auxin efflux in apical hook development of *Arabidopsis thaliana*. Development **137**: 607–617

Zhang W, To JP, Cheng CY, Schaller GE, Kieber JJ (2011) Type-A response regulators are required for proper root apical meristem function through post-transcriptional regulation of PIN auxin efflux carriers. Plant J **68**: 1–10